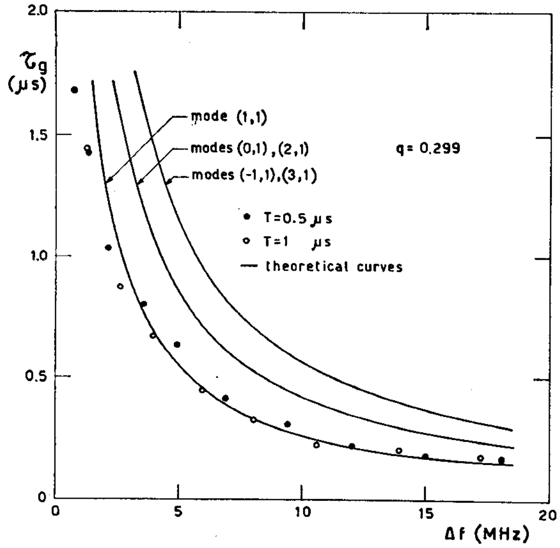

Fig. 3. Theoretical group delay (solid lines) versus frequency distance from cutoff for various modes and a given aspect ratio q. Dots are experimental values of the delay measured by the "gate" method.

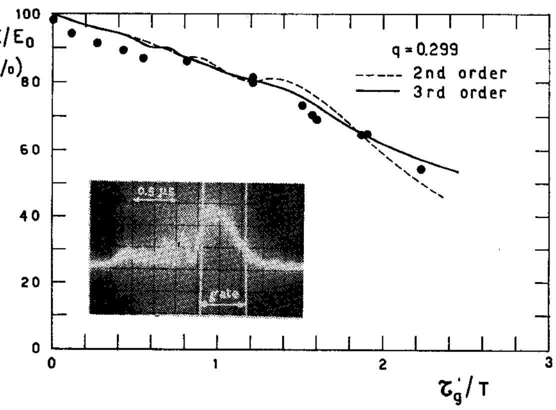

Fig. 4. Dispersion parameter E/E_0 versus reduced delay τ_g/T, for a given aspect ratio q, computed for two different approximations of (2). Dots are experimental data. The insert shows an example of pulse output when E/E_0 is 65 percent.

envelope is symmetrical, and symmetry is insured when the transfer function is symmetrical with respect to ω_0. This is, for instance, true of the linear case of footnote 3. In the case of the magnetostatic delay line, the experiments show the gate delay to closely correspond to the group delay as in the example of Fig. 3.[5] We can thus compare the theoretical results of E/E_0 at $t=\tau_g$, versus τ_g, with the measurements of (E/E_0)max versus the gate delay. This is shown in Fig. 4, where the third- and second-order approximations are both shown. The agreement between theory and experiment is satisfactory. The fact that the quadratic and cubic approximations give very similar results is true for the commonly used aspect ratios and for the quantity E/E_0 (not for the pulse shape).

From Fig. 4 we derive that even accepting an energy degradation around 50 percent, the delay is still only somewhat more than twice the pulse duration. Note that a degradation of this order appears to be rather extreme because one-half of the output energy is outside the original pulse duration. In practice a "delayed pulse" of this sort is hardly recognizable as a pulse. An example of delayed pulse corresponding to a 65-percent energy degradation is shown in the insert of Fig. 4.

Of course, using lower aspect ratios or higher modes (greater α) reduces dispersion, but the gain in delay for a given dispersion is not large, as can be derived from the α dependence of p_1 and p_2 and from Fig. 2. Computations and experiments with other aspect ratios confirm the behavior of Fig. 4 (e.g., with a $q=0.222$ and a 50-percent energy degradation the delay is still about $3T$).

[5] The excited mode was the (1, 1) mode, as indicated not only by Fig. 3, but also by previous measurements of dispersion curves [8] and by the output pulse shapes (e.g., Fig. 1).

III. Conclusions

On the basis of theoretical considerations and experiments it can be affirmed that the obtainable magnetostatic delay is limited, for normal aspect ratios, to about 3 times the pulse duration. Dispersion is the limiting factor; losses play a very minor role, as demonstrated by the fact that our theory, though lossless, agrees with the experiments satisfactorily.

Some improvement for practical signal-processing purposes might be obtained by reducing the harmonic content of the "delayed" pulse, either adopting a more suitable input pulse shape (e.g., Gaussian shape) or using suitable filtering techniques. Still, improvement amounts to a better display of the information available, not, of course, to a reduction of the transmission distortion.

Additionally, we suggest the energy degradation parameter E/E_0, as a convenient and physically meaningful parameter in dispersion problems. Also, the gate method has proved very effective for time-delay measurements in extreme dispersion situations, where leading and trailing edges, maxima, and 50-percent levels are no longer clearly identifiable.

References

[1] R. W. Damon and H. van de Vaart, "Propagation of magnetostatic spin waves at microwave frequencies, II rods," *J. Appl. Phys.*, vol. 37, p. 2445, 1966.
[2] R. I. Joseph and E. Schlömann, "Theory of magnetostatic modes in long axially magnetized cylinders," *J. Appl. Phys.*, vol. 32, p. 1001, 1961.
[3] A. Sommerfeld, *Electrodynamics*. New York: Academic Press, 1964, p. 82.
[4] M. Biri, L. Millanta, N. Rubino, and V. Tognetti, "A dispersive medium with cubic phase characteristic: Application to the magnetostatic delay line," Istituto di Ricerca sulle Onde Elettromagnetiche, Florence, Italy, Tech. Rep. 131-6-11, Jan. 1971.
[5] A. Abramowitz and I. A. Stegun, *Handbook of Mathematical Functions*. New York: Dover, 1965, p. 447.
[6] K. G. Budden, *Radio Waves in the Ionosphere*. Cambridge, England: Cambridge Univ. Press, 1966.
[7] E. R. Burke and S. M. Bhagat, "The propagation of magnetostatic spin waves in yttrium iron garnet," Univ. of Maryland, College Park, Tech. Rep. 760, 1967.
[8] M. Biri, L. Millanta, N. Rubino, and I. Kaufman, "Magnetostatic waves in axially magnetized cylinders: Experimental dispersion curves," *Nuovo Cimento*, vol. 47B, p. 281, 1967.

Electronic Tuning of the Punch-Through Injection Transit-Time (PITT) Microwave Oscillator

NIZAR B. SULTAN and G. T. WRIGHT

***Abstract*—Experimental results of the dynamic resistance and capacitance of p^+-n-p^+ punch-through injection transit-time (PITT or BARRITT) diodes are presented. A method of predicting the oscillator electronic tuning from the change in the device capacitance is outlined and verified experimentally at X band.**

Introduction

Experimental results of the microwave CW performance of the punch-through injection transit-time (PITT) oscillator have been reported recently [1]–[3]. A detailed small-signal design theory has been developed by Wright and Sultan [4] for the device under high-field conditions, taking into account the effects of diffusion and field dependence of carrier mobility. Here we present the experimental results of dynamic capacitance for a p^+-n-p^+ device as a function of frequency and current density. Later, it is shown how these results can be used to predict the performance of the electronic tuning. The latter was investigated at X band in a 7-mm coaxial cavity, and the results are discussed in terms of the change in dynamic capacitance.

Dynamic Impedance

The structure used was a silicon p^+-n-p^+ mesa device, with boron-diffused and evaporated gold contacts, a 4-$\Omega\cdot$cm epitaxial layer, a source to drain spacing of effectively 5 μm, and an active area of 1.2×10^{-4} cm^2. The devices were mounted in microwave S4 packages [6]. Small-signal measurements of the input impedance for the packaged devices were carried out with a computerized network analyzer. The diode dynamic impedance was deduced from these measurements using an equivalent circuit for the S4 package derived by Owens [5],

Manuscript received March 15, 1972; revised June 26, 1972. This work was supported by the Science Research Council and the Ministry of Technology.
N. B. Sultan was with the Department of Electronic and Electrical Engineering, University of Birmingham, Birmingham, England. He is now at P.O. Box 2771, Damascus, Syria.
G. T. Wright is with the Department of Electronic and Electrical Engineering, University of Birmingham, Birmingham, England.

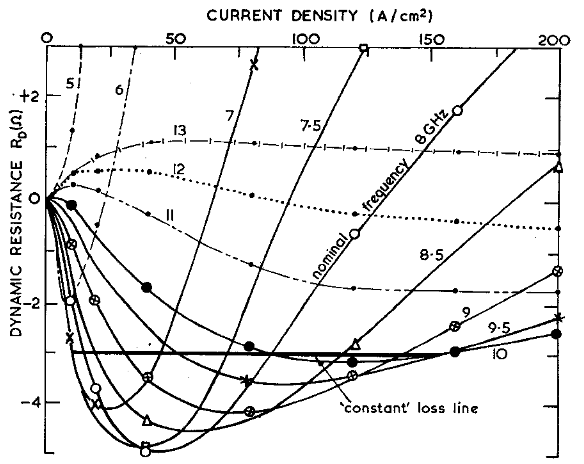

Fig. 1. Measured small-signal dynamic negative resistance of the diode versus bias current density, with nominal frequencies as parameters.

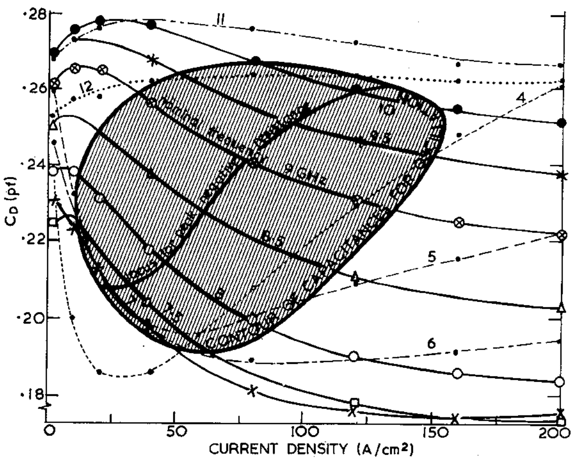

Fig. 2. Measured small-signal diode dynamic capacitance versus bias current density.

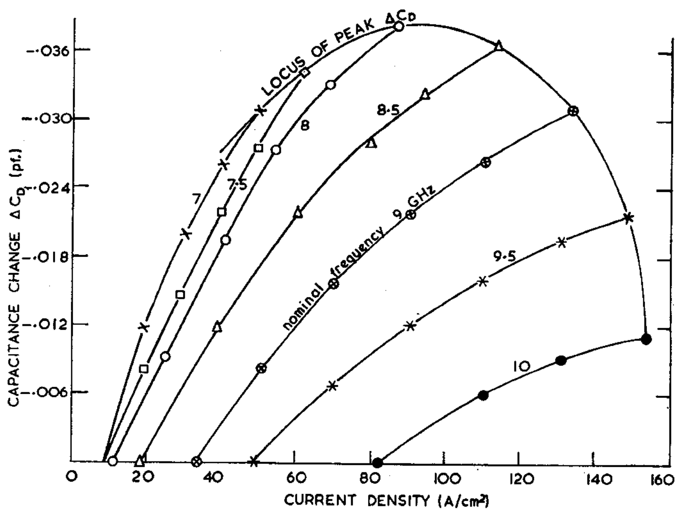

Fig. 3. Change in dynamic capacitance versus bias current density, within the contour of capacitances for oscillation.

but modified to fit the results of our own measurements on short-circuit and open-circuit packages.

Fig. 1 shows that the dynamic negative resistance occurs in the range of 6 to 12 GHz, and that for any one nominal frequency it can exist only over a certain range of bias current, the latter being different for different frequencies. However, the actual values of the net negative resistance and hence the effective range of frequencies and bias currents available under oscillation conditions are much smaller, due to device and cavity losses. A simplified approach would be to assume that these losses are constant. In this case we need only consider the net negative resistance values below a horizontal line of "constant loss," as shown in Fig. 1. Therefore, oscillation can only occur between 7 and 10 GHz. These observations agree satisfactorily with the oscillator performance.

The device losses are not included in Fig. 1. They are obtained by making use of the fact that, at the exact punch-through bias, the device behaves purely as a capacitor (equal to the diode geometric capacitance), and, therefore, the dynamic resistance is zero. Hence the resistance measured at punch-through, at the device terminals, represents the total diode and bonding wire losses.

The values of the device capacitance C_D have been derived between 4 and 12 GHz, from the same impedance measurements as above. At the punch-through bias of 21.0 V and 0.1 mA, C_D was found to lie between 0.23 and 0.28 pF, these values being comparable to the geometric capacitance of 0.26 pF for the device used. Fig. 2 shows how transit-time effects modify the dynamic capacitance at different current densities. These changes in the dynamic capacitance are caused by the transit-time delay of the space-charge current between source and drain. The consequent phase lag of the particle current with respect to voltage creates a component of reactive current which is in antiphase with the normal displacement current of the electrode capacitance. At certain transit angles and current densities, therefore, the electronic processes within the device create a negative capacitance as well as a negative resistance. This subtracts from the geometrical capacitance to produce a net capacitance which remains positive but which varies with frequency and bias current as shown in Fig. 2.

Prediction of Electronic Tuning

The above results indicate that for a given frequency lying within the oscillation range of 7 to 10 GHz the dynamic capacitance decreases as the bias current is increased. The rate of fall of this capacitance in picofarads per milliamperes decreases with increasing frequency and becomes practically zero at the upper frequency of oscillation. Similar performance has been obtained for n^+-p-n^+ structures.

Returning to Fig. 1, the results of available negative resistance below the "constant-loss" line provide the upper and lower limits of the bias current density necessary for electronic tuning, for each frequency of oscillation. These limits, indicated in Fig. 2, form the contour within which oscillation takes place. Therefore, it becomes possible to determine the range of useful capacitance change ΔC_D for a given center frequency and hence the range of resulting oscillation frequency change Δf. The locus of capacitance corresponding to the peak negative resistance is marked on the same diagram. Fig. 3 summarizes the result of the variation of the useful capacitance change ΔC_D with the current density.

The electronic tuning has been verified experimentally at X band with the 7-mm coaxial cavity described in [3]. By increasing the bias current while keeping the mechanical tuning conditions fixed, the oscillation frequency was found to increase as shown in Fig. 4(a). As the center frequency was increased from 7 to 10 GHz, the frequency range of the electronic tuning was found to possess a maximum value of typically 85 MHz at about 8 GHz, corresponding to a maximum useful capacitance change ΔC_D of 0.038 pF.

The current tuning range was found to increase from 1.6 to 16 mA, and the tuning sensitivity to decrease from typically 30 MHz/mA at 7 GHz to less than 3 MHz/mA at 10 GHz. The corresponding power level variations are shown in Fig. 4(b). The bias currents at which maximum oscillation power occurs are seen to coincide with those values corresponding to the peak negative resistance.

Fig. 4(a) and (b) shows that the electronic tuning linearity, sensitivity, and the corresponding bandwidth of power level can be designed by the proper choice of operating parameters. These results are important for some practical application in radar and communications, such as FM–CW radar and automatic frequency control, particularly since the PITT oscillator is basically a low-noise microwave source. Frequency modulation is possible using a linear and flat response.

In conclusion, the behavior of the dynamic capacitance of the

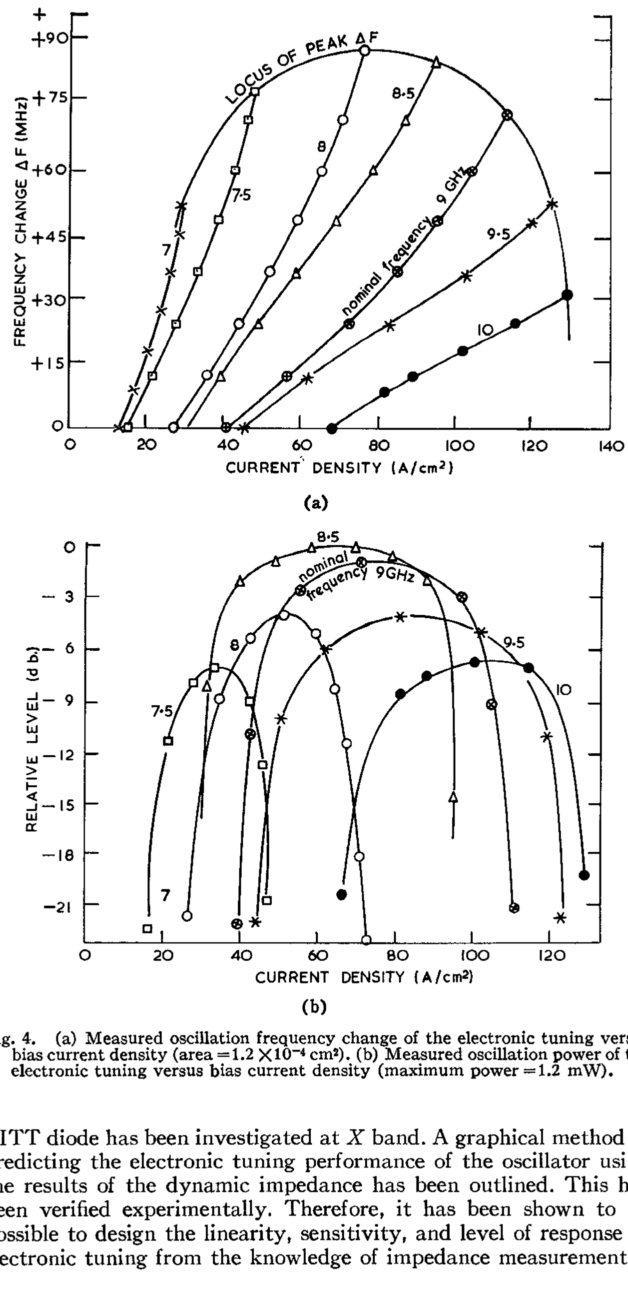

Fig. 4. (a) Measured oscillation frequency change of the electronic tuning versus bias current density (area $=1.2\times10^{-4}$ cm²). (b) Measured oscillation power of the electronic tuning versus bias current density (maximum power $=1.2$ mW).

PITT diode has been investigated at X band. A graphical method of predicting the electronic tuning performance of the oscillator using the results of the dynamic impedance has been outlined. This has been verified experimentally. Therefore, it has been shown to be possible to design the linearity, sensitivity, and level of response of electronic tuning from the knowledge of impedance measurements.[1]

Acknowledgment

The authors wish to thank J. Hinton and F. Smith for their help in the experimental work, L. Thompson and M. Cheley for the device fabrication, our colleagues at the Royal Radar Establishment, Malvern, for their assistance in device encapsulation, and, in particular, G. Parkes for his work on the automatic network analyzer.

References

[1] D. J. Coleman and S. M. Sze, "A low-noise metal–semiconductor–metal (MSM) microwave oscillator," *Bell Syst. Tech. J.*, vol. 50, pp. 1695–1699, 1971.

[2] C. P. Snapp and P. Weissglas, "Experimental comparison of silicon p-n-p and Cr-n-p transit-time oscillators," *Electron. Lett.*, vol. 7, pp. 743–744, 1971.

[3] N. B. Sultan and G. T. Wright, "The punch-through oscillator—New microwave solid-state source," *Electron Lett.*, vol. 8, pp. 24–26, 1972.

[4] G. T. Wright and N. B. Sultan, "Small-signal design theory and experiment for the microwave punch-through oscillator," to be published.

[5] R. P. Owens, "Mount-independent equivalent circuit of the S4 diode package," *Electron. Lett.*, vol. 7, pp. 580–582, 1971.

[6] R. P. Owens and D. Cawsey, "Microwave equivalent-circuit parameters of Gunn-effect-device packages," *IEEE Trans. Microwave Theory Tech.*, vol. MTT-18, pp. 790–798, Nov. 1970.

[1] For further details, refer to: N. B. Sultan, "The punch-through injection transit-time (PITT) diode, a new microwave oscillator," Ph.D. dissertation, Univ. of Birmingham, Birmingham, England, 1972.

Anisotropy in Alumina Substrates for Microstrip Circuits

J. H. C. van HEUVEN and T. H. A. M. VLEK

***Abstract*—By determining up to 16 GHz the effective dielectric constant for microstrip lines with various strip widths, it has been found that anisotropy in alumina substrates considerably affects the wavelength and is responsible for most of the discrepancy between theory and experiments.**

In the static theory originally presented by Wheeler [1], the concept of the effective dielectric constant (DC) (ϵ_{eff}) for microstrip lines has been introduced, assuming TEM wave propagation. Early experiments showed the existence of dispersion in microstrip lines. Numerous measurements of dispersion have been reported, mainly on 50-Ω lines on alumina substrates. The discrepancies, observed sometimes between experimental results, could not be explained by the inaccuracy of the measurements. The discrepancies can be partly explained by the difference in the relative DC (ϵ_r) of the substrate [3], [4]. During our measurements of ϵ_{eff} with various strip widths on alumina substrates, we found another cause for the discrepancy between static theory and measured data: anisotropy in the alumina substrates. Anisotropy is a well-known property of sapphire, i.e., a single crystal of aluminum oxide. In polycrystalline alumina a preferred orientation of the crystallites can sometimes be observed. In sapphire, the DC (ϵ_r) in the direction of the optic axis is 10.55 according to [5] or 11.5 according to [6]. For a few synthetic sapphire substrates we found $\epsilon_r=11.7$ (±1 percent), for which the supplier specified 10.55. Perpendicular to the optic axis, $\epsilon_r=8.6$ [5] or 9.5 [6]. For alumina without a preferred orientation, 9.7 is given in [5], which is the same value as specified by the supplier.

In this short paper experiments are described, showing clearly the effect of anisotropy on ϵ_{eff} of microstrip lines on alumina. For comparison, results with isotropic materials: fused quartz and nonmagnetic ferrite, having a lower (3.78) and a higher (13.9) ϵ_r than alumina, are given. The relevant properties of the substrates used are summarized in Table I. The values of ϵ_r are derived from capacitance measurements at 100 kHz.

A simple determination of ϵ_{eff} is obtained from capacitance measurements of microstrip line lengths with various strip widths at a sufficiently low frequency (100 kHz). Then ϵ_{eff} is defined as

$$\epsilon_{eff} = \frac{C_l}{C_0}$$

where C_l denotes the measured capacity of the line and C_0 the capacity of the line for substrates with $\epsilon_r=1$. The latter cannot be measured, but is derived from the characteristic impedance of a line for substrates with $\epsilon_r=1$ as given in [2]. Since $Z_0=(L/C_0)^{1/2}$ and $c=3.10^8$ m/s $=(LC_0)^{-1/2}$, ϵ_{eff} can be written as

$$\epsilon_{eff} = C_l \cdot c \cdot Z_0.$$

This value, denoted by ϵ_{eff} (*dc*), should equal that obtained from the static theory [2], denoted by ϵ_{eff} (*st*), within the accuracy of the approximation and that of the measurement (about 1 percent).

A second method was used for determining dispersion and for verifying the data ϵ_{eff} (*dc*) obtained from capacitance measurements. By measuring the resonance frequency of transmission-type resonators, consisting of lengths of coupled microstrip lines, the wavelength can be determined and ϵ_{eff} is found as

$$\epsilon_{eff}(w) = \left(\frac{\lambda_0(w)}{\lambda_g(w)}\right)^2$$

where $\lambda_0(w)$ and $\lambda_g(w)$ represent the wavelength in free space and in the microstrip line, respectively, at an angle frequency w. $\epsilon_{eff}(w)$ depends on frequency, indicating dispersion. Corrections Δl for the fringe fields at the open ends of the resonators are derived from measurements with resonant line lengths $l_1 \approx n_1\lambda_g(w_1)/2$ and $l_2 \approx n_2\lambda_g(w_2)/2$ where $n_{1,2}$ is a whole number and $w_1 \approx w_2$ [7]. The correction follows

Manuscript received March 31, 1972; revised June 29, 1972.

The authors are with Philips Research Laboratories, Eindhoven, The Netherlands.